An Asymptotic Solution for Surface Fields on a Dielectric-Coated Circular Cylinder with an Effective Impedance Boundary Condition

Andrés G. Aguilar, Zvonimir Sipus, and Manuel Sierra-Pérez

***Abstract*—An effective surface impedance approach is introduced for determining surface fields on an electrically large dielectric-coated metallic circular cylinder. Differences in analysis of rigorously-treated coated metallic cylinders and cylinders with an impedance boundary condition (IBC) are discussed. While for the impedance cylinder case a single constant surface impedance is considered, for the coated metallic cylinder case two surface impedances are derived. These are associated with the TM and TE creeping wave modes excited on a cylinder and depend on observation and source positions and orientations. With this in mind, a uniform theory of diffraction (UTD) based method with IBC is derived for the surface fields by taking into account the surface impedance variation. The asymptotic expansion is performed, via the Watson transformation, over the appropriate series representation of the Green's functions, thus avoiding higher-order derivatives of Fock-type integrals, and yielding a fast and an accurate solution. Numerical examples reveal a very good accuracy for large cylinders when the separation between the observation and the source point is large. Thus, this solution could be efficiently applied in mutual coupling analysis, along with the method of moments (MoM), of large conformal microstrip array antennas.**

***Index Terms*—Conformal antennas, electromagnetic coupling, Green function, uniform theory of diffraction, surface impedance.**

I. Introduction

CURRENT communication and radar systems have demanding requirements which lead to the development of new antenna structures. Conformal arrays may be an alternative to planar antennas because they can be integrated into curved surfaces offering large observation angles, low aerodynamic payload and aesthetic advantages. This makes conformal array antennas very attractive for satellite, aircraft, ship, land vehicle or cellular phone base station applications. As radiating elements printed antennas are often selected because of their low fabrication cost, light weight, ease of conformity on curved surfaces, and direct integrability with active devices.

Conformal array antennas can be divided in two categories [1]: those mounted on surfaces with electrically small or medium curvature radius, and those mounted on electrically large surfaces. Modal solutions in spectral domain are extensively used for analyzing canonical convex shapes such as circular or elliptic cylinders [2], [3], spheres [4] or cones [5], but as the surface radius increases a large number of terms are necessary, resulting in computationally intractable solutions. For electrically large structures the uniform theory of diffraction (UTD) [6], [7] can solve this type of problem. There are available solutions for canonical perfect electric conductor (PEC) surfaces, in some cases covered with a dielectric coating, and also for arbitrarily shaped surfaces. On the other hand, UTD does not support multilayer substrates and requires at least a moderate separation between source and observation points. An asymptotic solution for the surface fields on a dielectric-coated PEC circular cylinder has been developed in [8], [9], where Green's functions counterpart is evaluated via Watson transformation [10] in which Olver's and Debye's Hankel asymptotic approximations are implemented (instead of Watson's representation [11]). Recently, a new UTD based solution with an impedance boundary condition (IBC) has been introduced for evaluation of surface fields on circular cylinders [12], [13] and spheres [14], where a single constant surface impedance is considered. In these latter works, the asymptotic expansion is performed by considering the vector potentials and then by calculating higher-order derivatives of Fock-type integrals in order to obtain the fields.

In this paper, a UTD method with an effective IBC is proposed for efficient computation of surface fields on a thin coated metallic circular cylinder. The surface fields are characterized through accurate IBC in such a way that the surface impedance depends on the wave numbers, the substrate properties and the surface ray inclination. Two surface impedances are used in the formulation, associated with the TM and TE creeping wave modes excited on a cylinder. For this purpose a modified IBC is needed to accurately reproduce the coated case, which yields surface impedance correction terms that do not appear in classical IBC. Green's functions are then evaluated asymptotically avoiding higher-order derivatives of Fock-type of integrals, which can be computationally very demanding when surface impedance varies with the integration parameter. These Green's functions form the kernel of an electric field integral equation (EFIE) which, in combination with the method of moments (MoM), can be used to determine the mutual coupling between printed elements (e.g. patches). Only non-paraxial region has been considered, however the analysis method could be enhanced by implementing one of the asymptotic solutions valid within the paraxial region and available in the literature [15], [16]. Moreover, further study of analytic methods for the canonical problem of microstrip antennas on coated circular-cylindrical or spherical structures may lead toward the development of an efficient designing tool for patch arrays printed over large arbitrary convex coated surfaces [7].

The paper is organized as follows. In section II an effective

IBC is derived and a comparison between impedance cylinder and rigorously-treated coated metallic cylinder problem is performed. Section III describes the UTD with IBC Green's functions, including the dependency of the surface impedance on the spectral variables and the geometrical parameters. Numerical examples of mutual impedance between two printed elements, together with the limitations of the proposed effective IBC, are discussed in section IV. Conclusions are drawn and presented in the fifth section. An $e^{j\omega t}$ time dependence is assumed and suppressed throughout this paper.

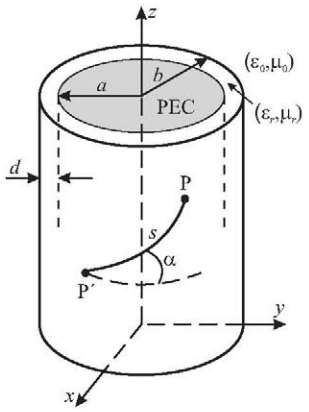

Fig. 1. Geometry of a surface field ray on an infinitely long dielectric-coated PEC circular cylinder.

II. Surface Impedance Characterization

The geometry of the problem is shown in Fig. 1, where an electric current source excites electromagnetic fields over the surface of an infinitely long PEC circular cylinder of radius a covered by a dielectric layer of thickness d. The mutual coupling analysis requires evaluation of the surface fields, where the boundary condition on the coated metallic surface can be approximated by an IBC if the surface fields are properly characterized. In other words, accurate IBC depends on frequency, substrate parameters and on the geodesic ray angle α from the source point P' to the observation point P.

Since Green's functions are derived in spectral domain, the following Fourier transform pair is defined:

$$f(\phi,z)=\frac{1}{2\pi}\sum_{n=-\infty}^{\infty}e^{jn\phi}\int_{-\infty}^{\infty}\tilde{F}(n,k_z)e^{jk_z z}dk_z \tag{1a}$$

$$\tilde{F}(n,k_z)=\frac{1}{2\pi}\int_0^{2\pi}\int_{-\infty}^{\infty}f(\phi,z)e^{-jk_z z}e^{-jn\phi}dz\ d\phi \tag{1b}$$

where $f(\phi,z)$ is any function in spatial domain and $\tilde{F}(n,k_z)$ in spectral domain.

In the surface impedance approach in the spatial domain the tangential surface fields satisfy the following IBC, as given by Leontovich [17], [18]

$$\hat{\rho}\times\vec{E}=Z_s\hat{\rho}\times(\hat{\rho}\times\vec{H})_{|\rho=b} \tag{2}$$

where Z_s is the surface impedance of the structure and $\hat{\rho}$ is the surface normal. This boundary condition can be written in matrix format as

$$\begin{bmatrix}E_\phi\\H_\phi\end{bmatrix}=\begin{bmatrix}-Z_s^e & 0\\0 & Y_s^m\end{bmatrix}\begin{bmatrix}H_z\\E_z\end{bmatrix}_{|\rho=b} \tag{3}$$

where Y_s^m and Z_s^e are defined as the TM and TE surface admittance and impedance, respectively. These effective IBC in (3) are useful to calculate the scattered field over any structure, provided that the surface admittance/impedance is characterized [19]. However, to determine the surface fields, the modal analysis of coated metallic cylinder shows that the rigorous IBC in the spectral domain are given by

$$\begin{bmatrix}\tilde{E}_\phi\\\tilde{H}_\phi\end{bmatrix}=\begin{bmatrix}-Z_s^e & -\frac{nk_z}{\rho k_{\rho 1}^2}\\-\frac{nk_z}{\rho k_{\rho 1}^2} & Y_s^m\end{bmatrix}\begin{bmatrix}\tilde{H}_z\\\tilde{E}_z\end{bmatrix}_{|\rho=b} \tag{4}$$

with n and k_z the azimuthal and axial wave numbers, respectively. Here $k_0=\omega\sqrt{\mu_0\varepsilon_0}$ and $k_1=k_0\sqrt{\mu_r\varepsilon_r}$ are the wave numbers in free space and within the dielectric, and $k_{\rho 0}^2=k_0^2-k_z^2$ and $k_{\rho 1}^2=k_1^2-k_z^2$ are the radial wave numbers in free space and inside the dielectric medium, respectively. These rigorous IBC for circular cylinders are derived from the relation between $\phi-$ and $z-$components of magnetic and electric fields in the substrate, given by

$$\tilde{H}_\phi=-j\frac{k_1Y_1}{k_{\rho 1}^2}\frac{\partial\tilde{E}_z}{\partial\rho}-\frac{nk_z}{\rho k_{\rho 1}^2}\tilde{H}_z \tag{5a}$$

$$\tilde{E}_\phi=-\frac{nk_z}{\rho k_{\rho 1}^2}\tilde{E}_z+j\frac{k_1Z_1}{k_{\rho 1}^2}\frac{\partial\tilde{H}_z}{\partial\rho} \tag{5b}$$

with $Z_1=\frac{1}{Y_1}=\sqrt{\frac{\mu_0\mu_r}{\varepsilon_0\varepsilon_r}}$ the characteristic impedance of the dielectric substrate. The boundary conditions in (3) are the planar approximation of (4), when $\rho\to\infty$.

The surface admittance and impedance (Y_s^m/Z_s^e) are normalized by $Z_0=\frac{1}{Y_0}=\sqrt{\frac{\mu_0}{\varepsilon_0}}$, characteristic impedance in free space, by defining

$$\Lambda_s^m\equiv\frac{Y_s^m}{Y_0}\ ,\quad \Lambda_s^e\equiv\frac{Z_s^e}{Z_0}\ . \tag{6}$$

This notation is going to be assumed in order to match the impedance cylinder problem with the dielectric-coated one, and will be justified later on. If a single constant surface impedance Z_s is considered then the boundary conditions in (3) are applied and

$$\Lambda_s^e=(\Lambda_s^m)^{-1}\equiv\Lambda_s=\frac{Z_s}{Z_0}\ . \tag{7}$$

When $\Lambda_s\to 0$ the non-coated PEC case is recovered.

By enforcing the rigorous IBC in (4), the vector potentials for outgoing waves can be expressed in terms of Hankel functions of second kind. Thus, for $\rho>b$

$$\tilde{A}_z(n,k_z) = -\frac{1}{k_{\rho 0}}\frac{1}{D_n}\frac{H_n^{(2)}(k_{\rho 0}\rho)}{H_n^{(2)}(k_{\rho 0}b)}\cdot$$
$$\cdot\left\{\left(R_n+\frac{q_e}{m_t}\right)\tilde{J}_z - j\frac{k_0 k_{\rho 0}}{k_1^2-k_0^2}\frac{q_c}{m_t}\left(R_n+\frac{k_{\rho 1}^2}{k_{\rho 0}^2}\frac{q_e}{m_t}\right)\tilde{J}_\phi\right\} \tag{8a}$$

$$\tilde{F}_z(n,k_z) = -\frac{Z_0}{k_{\rho 0}}\frac{1}{D_n}\frac{H_n^{(2)}(k_{\rho 0}\rho)}{H_n^{(2)}(k_{\rho 0}b)}\left\{\frac{q_c}{m_t}\tilde{J}_z + \right.$$
$$\left. + j\frac{k_0}{k_{\rho 0}}\left[\frac{q_e}{m_t}\left(R_n+\frac{q_m}{m_t}\right) - \frac{k_{\rho 0}^2}{k_1^2-k_0^2}\left(\frac{q_c}{m_t}\right)^2\right]\tilde{J}_\phi\right\} \tag{8b}$$

where $\tilde{J}(n,k_z) = \tilde{J}_\phi\hat{\phi} + \tilde{J}_z\hat{z}$ is the tangential current distribution over the cylinder surface in spectral domain.

The factor m_t is defined as $m_t = \left(\frac{k_{\rho 0}b}{2}\right)^{1/3}$. Moreover, expression D_n in the denominator is given by

$$D_n = \left(R_n+\frac{q_e}{m_t}\right)\left(R_n+\frac{q_m}{m_t}\right) + \left(\frac{q_c}{m_t}\right)^2 \tag{9}$$

and

$$R_n = \frac{H_n^{(2)\prime}(k_{\rho 0}b)}{H_n^{(2)}(k_{\rho 0}b)} \tag{10}$$

with $H_n^{(2)}(z)$ and $H_n^{(2)\prime}(z)$ the Hankel function of second kind and its first derivative with respect to its argument, respectively. It is noted that the factor m_t could be removed from previous equations, but it is included for subsequent convenience in the asymptotic expansion.

The Green's function $\tilde{G}_{uv'}$ in spectral domain, representing a $\hat{u}$-directed surface electric field due to a $\hat{v}'$-directed electric source point, is expressed as

$$\tilde{G}_{zz'}(n,k_z) = jZ_0\frac{k_{\rho 0}}{k_0}\frac{R_n+\frac{q_e}{m_t}}{D_n} \tag{11a}$$

$$\tilde{G}_{z\phi'}(n,k_z) = \tilde{G}_{\phi z'}(n,k_z) = Z_0\frac{\frac{q_c}{m_t}\frac{\tilde{q}_e^{z\phi}}{m_t}}{D_n} \tag{11b}$$

$$\tilde{G}_{\phi\phi'}(n,k_z) = -jZ_0\frac{k_0}{k_{\rho 0}}\frac{\frac{q_e}{m_t}R_n\left(R_n+\frac{q_m}{m_t}\right)+\left(\frac{q_c}{m_t}\right)^2\frac{\tilde{q}_e^{\phi\phi}}{m_t}}{D_n}\ , \tag{11c}$$

and are written in this format in order to be valid for either non-corrected (3) or rigorous (4) IBC. The differences in both problems come from the q factors. If an impedance circular cylinder is considered with a constant surface impedance, then

$$q_m = -jm_t\frac{k_{\rho 0}}{k_0}\Lambda_s^m \tag{12a}$$

$$q_e = \tilde{q}_e^{z\phi} = \tilde{q}_e^{\phi\phi} = -jm_t\frac{k_{\rho 0}}{k_0}\Lambda_s^e \tag{12b}$$

$$q_c(n,k_z) = -jm_t\frac{nk_z}{k_0 k_{\rho 0}b}\ . \tag{12c}$$

Note that the Green's functions in (11) through (12) are dual of the ones appearing in [12].

If the dielectric-coated PEC circular cylinder is rigorously treated, the Green's functions are the same than in (11) but with

$$q_m(n,k_z) = -jm_t\frac{k_{\rho 0}}{k_0}\cdot$$
$$\cdot\left(-j\frac{\varepsilon_r k_0}{k_{\rho 1}}\frac{J_n(k_{\rho 1}a)Y_n'(k_{\rho 1}b) - J_n'(k_{\rho 1}b)Y_n(k_{\rho 1}a)}{J_n(k_{\rho 1}a)Y_n(k_{\rho 1}b) - J_n(k_{\rho 1}b)Y_n(k_{\rho 1}a)}\right) \tag{13a}$$

$$q_e(n,k_z) = -jm_t\frac{k_{\rho 0}}{k_0}\cdot$$
$$\cdot\left(-j\frac{\mu_r k_0}{k_{\rho 1}}\frac{J_n'(k_{\rho 1}a)Y_n'(k_{\rho 1}b) - J_n'(k_{\rho 1}b)Y_n'(k_{\rho 1}a)}{J_n'(k_{\rho 1}a)Y_n(k_{\rho 1}b) - J_n(k_{\rho 1}b)Y_n'(k_{\rho 1}a)}\right) \tag{13b}$$

$$\tilde{q}_e^{z\phi}(n,k_z) = -jm_t\frac{k_{\rho 0}}{k_0}\cdot$$
$$\cdot\left[j\frac{k_{\rho 0}k_0}{k_1^2-k_0^2}\left(R_n+\frac{k_{\rho 1}^2}{k_{\rho 0}^2}\frac{q_e(n,k_z)}{m_t}\right)\right] \tag{13c}$$

$$\tilde{q}_e^{\phi\phi}(n,k_z) = -jm_t\frac{k_{\rho 0}}{k_0}\cdot$$
$$\cdot\left[j\frac{k_{\rho 0}^3k_0}{(k_1^2-k_0^2)^2}\left(R_n+\frac{k_{\rho 1}^4}{k_{\rho 0}^4}\frac{q_e(n,k_z)}{m_t}\right)\right] \tag{13d}$$

$$q_c(n,k_z) = -jm_t\frac{nk_z}{k_0k_{\rho 0}b}\frac{k_1^2-k_0^2}{k_{\rho 1}^2}\ . \tag{13e}$$

$J_n(z)$ and $Y_n(z)$ are Bessel functions of first and second kind, respectively, and $J_n'(z)$ and $Y_n'(z)$ denote their first derivative with respect to the argument.

Here q_m and q_e represent the surface impedance dependency for the TM and TE creeping waves excited on a cylinder, respectively, coupled through the q_c term. Differences in expressions of the surface field for the impedance and the metallic-coated circular cylinder are in $q_{m,e}$ and q_c parameters, except for a correction in the TE surface impedance, which depends also on the field and source orientation and is expressed through the factors $\tilde{q}_e^{z\phi}$ and $\tilde{q}_e^{\phi\phi}$. Such effect does not appear in the scattering problem.

In the limit case, when the surface ray inclination α (angle between the geodesic ray and the azimuthal direction) is zero, i.e. when $k_z = 0$, there is no torsion in surface fields and the coupling factor is $\lim_{\alpha\to 0^o} q_c(n,k_z) = 0$. Thus, Green's functions in (11) yield

$$\lim_{\alpha\to 0^o}\tilde{G}_{zz'} = jZ_0\frac{k_{\rho 0}}{k_0}\frac{1}{R_n+\frac{q_m}{m_t}} \tag{14a}$$

$$\lim_{\alpha\to 0^o}\tilde{G}_{z\phi'} = \lim_{\alpha\to 0^o}\tilde{G}_{\phi z'} = 0 \tag{14b}$$

$$\lim_{\alpha\to 0^o}\tilde{G}_{\phi\phi'} = -jZ_0\frac{k_0}{k_{\rho 0}}\frac{\frac{q_e}{m_t}R_n}{R_n+\frac{q_e}{m_t}}\ . \tag{14c}$$

Consequently, when $\alpha = 0^o$, the zz' and $\phi\phi'$ field components only depend on the TM and TE surface impedance (with no need of correction), respectively, while the $z\phi'$ and $\phi z'$ components vanish. However, when $\alpha \neq 0^o$ both set of modes

are coupled through the q_c factor, which is stronger as the angle α increases.

Therefore, if we would like to derive the surface field on a coated PEC circular cylinder with an equivalent IBC, the effective surface impedance must change with the substrate permittivity and permeability, with the ray angle α and depend on spectral variables n and k_z. It is obvious that by making a comparison between the coated and the impedance cylinder problems, the normalized surface admittance and impedance can be written as

$$\Lambda_s^m(n,k_z) = -j\frac{\varepsilon_r k_0}{k_{\rho 1}} \frac{J_n(k_{\rho 1}a)Y_n'(k_{\rho 1}b) - J_n'(k_{\rho 1}b)Y_n(k_{\rho 1}a)}{J_n(k_{\rho 1}a)Y_n(k_{\rho 1}b) - J_n(k_{\rho 1}b)Y_n(k_{\rho 1}a)} \tag{15a}$$

$$\Lambda_s^e(n,k_z) = -j\frac{\mu_r k_0}{k_{\rho 1}} \frac{J_n'(k_{\rho 1}a)Y_n'(k_{\rho 1}b) - J_n'(k_{\rho 1}b)Y_n'(k_{\rho 1}a)}{J_n'(k_{\rho 1}a)Y_n(k_{\rho 1}b) - J_n(k_{\rho 1}b)Y_n'(k_{\rho 1}a)} \tag{15b}$$

These expressions can also be derived if the surface admittance and impedance are calculated as the ratio of electric and magnetic field within the dielectric slab, by assuming no coupling between TM and TE modes, and applying the boundary conditions over the conducting cylinder.

For the $z\phi'/\phi z'$ and $\phi\phi'$ field and source components, the corrected TE surface impedance is

$$\tilde{\Lambda}_s^{e,z\phi}(n,k_z) = j\frac{k_{\rho 0}k_0}{k_1^2 - k_0^2}\left(R_n + \frac{k_{\rho 1}^2}{k_{\rho 0}^2}\frac{q_e(n,k_z)}{m_t}\right) \tag{16a}$$

$$\tilde{\Lambda}_s^{e,\phi\phi}(n,k_z) = j\frac{k_{\rho 0}^3 k_0}{(k_1^2 - k_0^2)^2}\left(R_n + \frac{k_{\rho 1}^4}{k_{\rho 0}^4}\frac{q_e(n,k_z)}{m_t}\right) \tag{16b}$$

This corrected TE surface impedance is essential for accurate modelling a dielectric coating through IBC. It does not influence the surface fields for $\alpha = 0^o$, but its effect increases as α does. Therefore, its presence is a consequence of the surface ray torsion along the geodesic paths on cylindrical bodies [7].

In addition, the q_c factor in equation (13e) can be written as the constant surface impedance coupling factor in (12c) multiplied by an extra term that describes the dielectric properties.

The surface impedance expressions in (15) and (16) are not suitable to be used in the UTD formulation, when Bessel and Hankel functions are of complex order. Thus, to simplify (15), two-term Debye's asymptotic formulas [20] are implemented and, as proposed in [21], a Taylor Series expansion in the $1/b$ variable around $1/b = 0$ is performed retaining the first two terms. Thus, the final form of the normalized surface admittance/impedance is given by

$$\Lambda_s^m(\nu,k_z) \sim -j\frac{\varepsilon_r k_0}{k_{\rho 1}^2}\left[\frac{\sqrt{k_{\rho 1}^2 - (\nu/b)^2}}{\tan\left(d\sqrt{k_{\rho 1}^2 - (\nu/b)^2}\right)} + \right.$$
$$\left. + \frac{1}{2b}\left(\frac{d^2(\nu/b)^2}{\sin^2\left(d\sqrt{k_{\rho 1}^2 - (\nu/b)^2}\right)} - \frac{k_{\rho 1}^2}{k_{\rho 1}^2 - (\nu/b)^2}\right)\right] \tag{17a}$$

$$\Lambda_s^e(\nu,k_z) \sim j\frac{\mu_r k_0}{k_{\rho 1}^2}\left[\sqrt{k_{\rho 1}^2 - (\nu/b)^2}\cdot\right.$$
$$\cdot \tan\left(d\sqrt{k_{\rho 1}^2 - (\nu/b)^2}\right) - \frac{1}{2b}\left(\frac{d^2(\nu/b)^2}{\cos^2\left(d\sqrt{k_{\rho 1}^2 - (\nu/b)^2}\right)} + \right.$$
$$\left.\left. + \frac{k_{\rho 1}^2}{k_{\rho 1}^2 - (\nu/b)^2}\tan^2\left(d\sqrt{k_{\rho 1}^2 - (\nu/b)^2}\right)\right)\right] \tag{17b}$$

where the azimuthal wave number n has been replaced by ν. This *Debye's approach* is shown to be accurate and efficient for all complex ν and k_z values for a thin dielectric layer. Although, strictly speaking, the Debye's asymptotic approximations used here are only valid for $|\nu| > |k_{\rho 1}a|$ and $|\nu| > |k_{\rho 1}b|$, they work very well for b close to a, even outside these limits, since expressions (15) are ratios of Bessel functions. Moreover, it is easily recognized that formulas in (17) can be split in two parts, as the surface impedance of a planar dielectric slab plus a curvature correction for the cylindrical problem.

Further approximations can be made to expressions in (17), if the first term is retained (planar approximation) and a *small argument* approximation is applied to the tangent function, which is true when the cylinder radius is very large and the dielectric thickness is very small, respectively,

$$\Lambda_s^m(\nu,k_z) \sim -j\frac{\varepsilon_r k_0}{k_{\rho 1}^2}\frac{1}{d} \tag{18a}$$

$$\Lambda_s^e(\nu,k_z) \sim j\frac{\mu_r k_0}{k_{\rho 1}^2} d\left(k_{\rho 1}^2 - (\nu/b)^2\right) \ . \tag{18b}$$

In this case, Λ_s^m becomes a constant for a given geometry, highlighting the low sensitivity to TM surface admittance variations.

In the problem at hand, the observation point lays in the shadow part of transition region with respect to the source. The scattered field on a coated PEC circular cylinder in the deep shadow region could be calculated through the Cauchy residue series on the ν-complex plane [19]. Although, in the transition region many poles would be necessary to consider to make the series convergent, the main field contribution comes from the first creeping wave mode ν_1, which is the first root of the transcendental equation in (9), i.e. $D_{\nu_1} = 0$. Therefore, for a given geometry, a *constant surface impedance* can be obtained by substituting ν_1 in (17) (or in (18)) and in (16). In the UTD formulation, the axial wave number k_z only depend on the surface ray inclination α. Thus, with a constant TM and TE surface impedance, the solution presented in [12], [13] could be effectively applied when a dielectric coating is present, but introducing the corrected TE surface impedance in (16). The nature of the poles on the complex ν-plane and the root searching are discussed in next section.

Since, in the transition region, it can be assumed $\nu \sim O(k_{\rho 0}b)$, the function (10) can be mapped by applying Watson's approximation for Hankel functions [11], as $R_n \sim -R_w/m_t$, with $R_w = W_2'(\tau)/W_2(\tau)$. Here, $W_2(\tau)$ and $W_2'(\tau)$ are a Fock-type Airy function and its first derivative, respectively, obtained through Fock substitution [22]:

$\nu = k_{\rho 0} b + m_t \tau$. Thus, the corrected TE surface impedances in (16) can be expressed asymptotically as

$$\tilde{\Lambda}_s^{e,z\phi}(\nu, k_z) \sim \frac{-j}{m_t} \frac{k_{\rho 0} k_0}{k_1^2 - k_0^2} \left(R_w + j m_t \frac{k_{\rho 1}^2}{k_0 k_{\rho 0}} \Lambda_s^e(\nu, k_z) \right) \tag{19a}$$

$$\tilde{\Lambda}_s^{e,\phi\phi}(\nu, k_z) \sim \frac{-j}{m_t} \frac{k_{\rho 0}^3 k_0}{(k_1^2 - k_0^2)^2} \left(R_w + j m_t \frac{k_{\rho 1}^4}{k_0 k_{\rho 0}^3} \Lambda_s^e(\nu, k_z) \right) \tag{19b}$$

with Λ_s^e containing the asymptotic surface impedance expression in (17b) or in (18b).

III. UTD Based Asymptotic Formulation

An elementary electric current source $\vec{P}^e = P_{\phi'}^e \hat{\phi}' + P_{z'}^e \hat{z}'$ is considered at $P' \equiv (b, \phi', z')$ placed on a dielectric-coated or on an impedance circular cylinder. The surface electric field at $P \equiv (b, \phi, z)$ in spatial domain can be expressed as

$$\vec{E}_t(\phi, z) = \frac{1}{4\pi^2 b} \sum_{n=-\infty}^{\infty} e^{jn\phi_d} \int_{-\infty}^{\infty} \underline{\underline{\tilde{G}_t}}(n, k_z) \cdot \vec{P}^e e^{jk_z z_d} dk_z \tag{20}$$

with $\phi_d = \phi - \phi'$ and $z_d = z - z'$. The dyadic Green's function $\underline{\underline{\tilde{G}_t}}$ contains the tangential electric field components in spectral domain due to a unitary electric source $\vec{P}^e$.

The electric field in (20) is expanded asymptotically by applying Watson transformation [10]. Then, the Green's functions in spatial domain for the l-th surface ray over the cylinder are written as

$$G_{uv'}^{l\pm}(\phi, z) = \frac{1}{4\pi^2 b} \int_{-\infty}^{\infty} e^{jk_z z_d} dk_z \cdot \cdot \int_{-\infty}^{\infty} \tilde{G}_{uv'}(\nu, k_z) e^{-j\nu\phi_l^{\pm}} d\nu \tag{21}$$

where sign $\pm$ indicates a clockwise or a counterclockwise geodesic ray $\phi_l^{\pm} = \pm(\phi_d - \pi) + (2l+1)\pi$. After Fock substitution [22], a polar change of variable is applied ($k_{\rho 0} = k_0 \cos\alpha$ and $k_z = k_0 \sin\alpha$), and the k_z-integration is performed through the steepest descent path method. Thus, the UTD with IBC Green's functions in the spatial domain for the l-th surface ray at $\rho = b$ are given by

$$G_{zz'}^{l\pm}(\phi, z) \sim G_0 \tilde{P}_m(\xi, \tau) \cos^2\alpha \tag{22a}$$

$$G_{z\phi'}^{l\pm}(\phi, z) = G_{\phi z'}^{l\pm}(\phi, z) \sim \pm G_0 \tilde{P}_c^{z\phi}(\xi, \tau) \frac{1}{k_0 s \cos\alpha} \tag{22b}$$

$$G_{\phi\phi'}^{l\pm}(\phi, z) \sim G_0 \left(\tilde{P}_e(\xi, \tau) + \tilde{P}_c^{\phi\phi}(\xi, \tau) \right) \frac{j}{k_0 s \cos^2\alpha} \tag{22c}$$

The function G_0 is the Green's function in free space

$$G_0 = -\frac{j Z_0 k_0}{2\pi} \frac{e^{-jk_0 s}}{s} \ . \tag{23}$$

The total dyadic Green's function for surface electric field is a summation of the all ray field contributions, although typically, only the first surface ray is enough for sufficiently large radii cylinders.

The geometrical parameters of the structure are defined in Fig. 1, where s is the length of the geodesic ray from the source to the observation point, and α is the angle between this ray and the circumferential direction. The functions $\tilde{P}_{m,e}$ and $\tilde{P}_c^{z\phi,\phi\phi}$ are the TM/TE and coupled Fock-type integrals, defined as

$$\tilde{P}_m(\xi, \tau) = \frac{1}{2} \sqrt{\frac{j\xi}{\pi}} \int_{-\infty}^{\infty} \frac{R_w - q_e(\tau)}{D_w} e^{-j\xi\tau} d\tau \tag{24a}$$

$$\tilde{P}_e(\xi, \tau) = -j\xi \sqrt{\frac{j\xi}{\pi}} \int_{-\infty}^{\infty} q_e(\tau) R_w \frac{R_w - q_m(\tau)}{D_w} e^{-j\xi\tau} d\tau \tag{24b}$$

$$\tilde{P}_c^{z\phi}(\xi, \tau) = j\xi m_t \sqrt{\frac{j\xi}{\pi}} \int_{-\infty}^{\infty} \frac{q_c(\tau) \tilde{q}_e^{z\phi}(\tau)}{D_w} e^{-j\xi\tau} d\tau \tag{24c}$$

$$\tilde{P}_c^{\phi\phi}(\xi, \tau) = -j\xi \sqrt{\frac{j\xi}{\pi}} \int_{-\infty}^{\infty} \frac{q_c^2(\tau) \tilde{q}_e^{\phi\phi}(\tau)}{D_w} e^{-j\xi\tau} d\tau \tag{24d}$$

where $\xi = m_t \phi_l^{\pm}$, R_w is already defined as a ratio of Fock-type Airy functions, and expression D_w is defined as

$$D_w(\tau) = (R_w - q_e(\tau))(R_w - q_m(\tau)) + q_c^2(\tau) \tag{25}$$

The functions $q_{m,e}$, $\tilde{q}_e$ and q_c are given by

$$q_{m,e}(\tau) = -j m_t \ \Lambda_s^{m,e}(\nu, k_z) \cos\alpha \tag{26a}$$

$$\tilde{q}_e(\tau) = -j m_t \ \tilde{\Lambda}_s^e(\nu, k_z) \cos\alpha \tag{26b}$$

$$q_c^{ibc}(\tau) = -j m_t \left(1 + \frac{\tau}{2m_t^2} \right) \sin\alpha \tag{26c}$$

$$q_c^{coated}(\tau) = q_c^{ibc}(\tau) \left(\frac{\mu_r \varepsilon_r - 1}{\mu_r \varepsilon_r - \sin^2\alpha} \right) \tag{26d}$$

where superscript ibc refers to the impedance cylinder case with the non-corrected IBC in (3), and with the single constant surface impedance as in (7); and $coated$ to the dielectric coating case with the rigorous IBC in (4), and with the TM/TE surface admittance/impedance as in (17) or in (18), corrected by (19), which could be constant if the first creeping wave pole of the cylinder is found.

The pole location can be determined by finding the roots of the transcendental equation in (25). Poles associated to highly attenuated creeping waves along the cylinder (or Watson modes) are located in the fourth quadrant of the complex τ-plane and appear in the vicinity of the Stokes line [23]. When the cylinder radius is large and/or the coating layer is thick, some of these poles may move toward the real axis, matching the surface waves (or Elliot modes) of an equivalent grounded planar dielectric slab. Typically, creeping waves are highly attenuated along the azimuthal direction, while surface waves experiment a low attenuation rate along ϕ direction. In the surface field problem, the first pole corresponds to an Elliot type mode and its field contribution is more important as the coating thickness increases or the cylinder radius grows. Thus, the second mode contribution is bigger for a thin substrate and a small cylinder.

A numerical procedure is implemented to find the first mode τ_1, i.e. $D_w(\tau_1) = 0$, which is necessary if a constant surface impedance is required. Initially, the first uncoupled TE mode is determined by calculating the first root of $W_2'(\tau) - q_e(\tau)W_2(\tau) = 0$, and by using as initial guess the first zero of the first derivative of the Airy function $Ai'(\tau e^{-j2\pi/3})$ [20]. Then, the first root of (25) is found, with the initial guess corresponding to the uncoupled TE mode calculated previously. For the root searching the Newton-Raphson's method is applied [20].

Fock-type integrals in (24) can be performed efficiently through numerical integration by deforming the integration path on the complex τ-plane [13], as can be seen in Fig. 2, and by using a Gauss quadrature. In the integral contour deformation, the value of τ_b must be large enough to guarantee that all poles are captured inside the integration contour. For all examples shown in section IV $\tau_b = 0.7k_0b$.

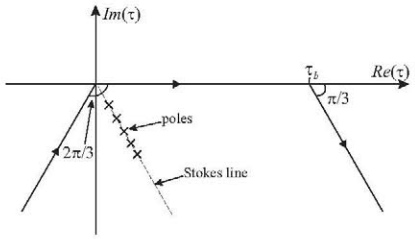

Fig. 2. Deformed integration path and pole location on the complex τ-plane.

IV. Mutual Impedance Results and Discussion

The geometry of two rectangular printed elements over a dielectric-coated grounded cylinder is shown in Fig. 3. The mutual coupling of these two patches can be evaluated through an EFIE-MoM formulation (Galerkin approach). Then, the MoM impedance matrix elements in spatial domain are given by

$$Z_{ji}(\phi_c, z_c) = \int_{S'}\int_{S} \vec{W}_j(\phi, z) \cdot \cdot \underline{\underline{G_t}}(\phi_c + \phi - \phi', z_c + z - z') \cdot \vec{J}_i(\phi', z')\, dS' dS \quad (27)$$

where (ϕ_c, z_c) is the distance between patch centers and $\underline{\underline{G_t}}$ is, in this case, the asymptotic dyadic Green's functions in spatial domain expressed by means of (22).

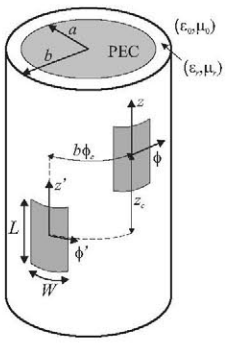

Fig. 3. Geometry of printed elements on a dielectric-coated PEC circular cylinder.

To estimate the accuracy of the surface field asymptotic representation, we have calculated the mutual impedance between two identical tangential electric current modes located at the surface of a dielectric-coated cylinder. The electric current distribution is assumed to be sinusoidal along the direction of the current and constant in the perpendicular direction. Such choice of current distribution guarantees the convergence of the eigenfunction reference solution in (20) for large cylinders, even though it is very slow. Only the first ray mode contribution ($l = 0$ and sign $+$) is necessary for the considered configurations.

Results are shown in Fig. 4 for the real and imaginary parts of the mutual impedance for different current orientations and α angles, along a geodesic ray around the cylinder, by using two surface impedance approaches: the Debye's surface impedance formula in (17) and the constant surface impedance obtained through the same Debye's formula particularized with the first creeping wave mode ν_1. A very good agreement is met when the geodesic length s is above $1\lambda_0$ for the Debye's approach case and above $2\lambda_0$ for the constant surface impedance.

Fig. 5 shows the amplitude of the mutual impedance between two ϕ-directed electric currents as a function of the geodesic ray angle α, for different distances s. Results for the other source and field orientations are similar. Here, the results obtained with the small-argument approximation of surface impedance in (18) are also included. The three surface impedance approaches are very accurate when $s \geq 2\lambda_0$, and they all fail in the vicinity of paraxial region (for $\alpha > 70^o$). Moreover, the non-corrected UTD result, which refers to the coated PEC case when $\tilde{\Lambda}_s^{e,z\phi} = \tilde{\Lambda}_s^{e,\phi\phi} = \Lambda_s^e$, i.e. without using the corrected TE surface impedance in (19), shows the importance of including these correction terms (only $s = 3\lambda_0$ is shown). Their effect are associated with the torsion of rays along the cylinder that tend to vanish when $\alpha \to 0^o$, as observed in Fig. 5.

Fig. 6 gives the amplitude of the mutual impedance between two ϕ-directed electric currents as a function of the dielectric thickness d, for a fixed geodesic ray angle α and length s. The Debye's approach losses accuracy for a dielectric thickness greater than $0.15\lambda_0$. The small-argument approximation remains accurate enough provided that the dielectric thickness d is lower than $0.1\lambda_0$. The constant surface impedance follows the Debye's formula behavior up to $0.07\lambda_0$; above this threshold the Elliot mode becomes very strong and other poles may move close to the real axis, whose contribution can not be neglected. The non-corrected solution becomes valid as $d \to 0$, where the PEC case is recovered.

In addition, Fig. 7 shows the amplitude of the mutual impedance between two ϕ-directed electric currents as a function of the grounded cylinder radius a, for a fixed coating thickness d, geodesic ray angle α and length s. A large discrepancy is found between the non-corrected and the other surface impedance approaches, even though the correction terms were supposed to be neglected for a large cylinder radius $\rho \to \infty$. One can conclude that such approximation is not valid and the correction factors are necessary even for very large cylinders. For the rest of surface impedance approaches,

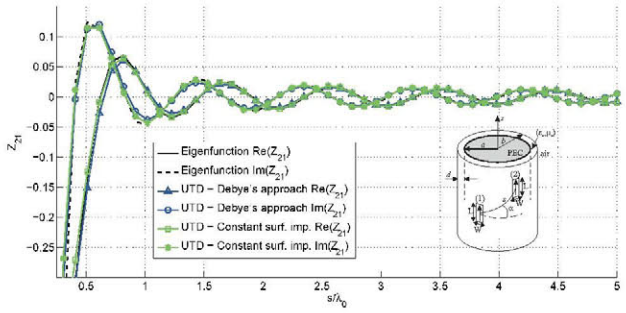

(a) Between two z-directed electric currents, $\alpha = 40^{\circ}$.

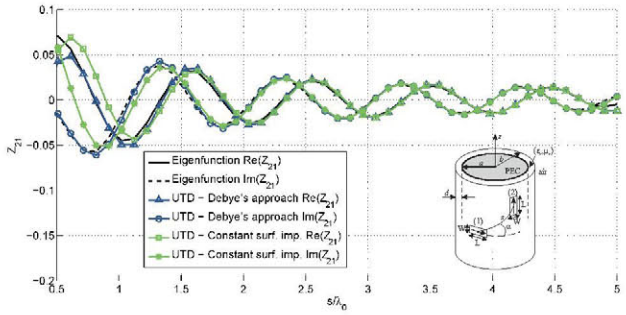

(b) Between a z- and a ϕ-directed electric currents, $\alpha = 55^{\circ}$.

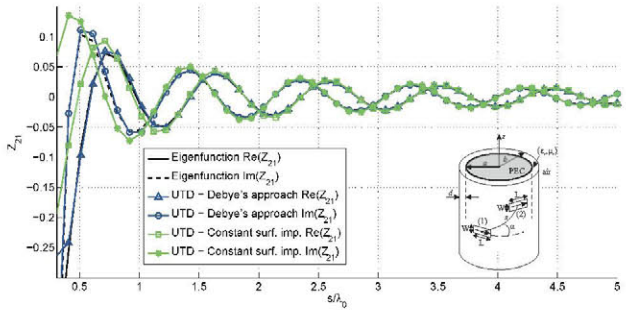

(c) Between two ϕ-directed electric currents, $\alpha = 25^{\circ}$.

Fig. 4. Mutual impedance between two electric currents on a dielectric-coated PEC circular cylinder as a function of s, with $\varepsilon_r = 2$, $\mu_r = 1$, $b = 5\lambda_0$, $d = 0.07\lambda_0$, $W = 0.1\lambda_0$ and $L = 0.1\lambda_0$.

the error between the UTD and the eigenfunction solution is low.

Finally, Fig. 8 shows the amplitude of the mutual impedance between two ϕ-directed electric currents as a function of the substrate relative permittivity ε_r, for a thin coating $d = 0.02\lambda_0$ and a fixed geodesic ray angle α and length s. The UTD solution with the three surface impedance approaches losses some accuracy as the relative permittivity grows, but this discrepancy is not very severe. As expected, the non-corrected case converges to the reference solution as $\varepsilon_r \to 1$.

V. Conclusion

A novel UTD-IBC method was presented which allows the calculation of surface fields over a thin dielectric-coated PEC circular cylinder. The TM and TE surface impedances can be seen as a contribution of the different TM/TE creeping wave modes excited on the cylinder, which are coupled when the

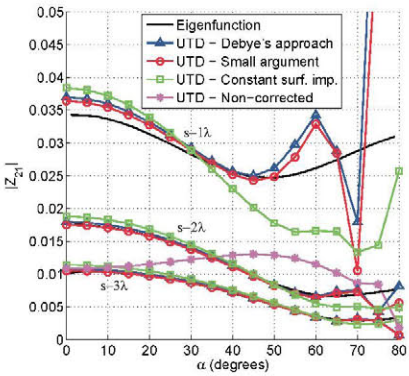

Fig. 5. Mutual impedance between two ϕ-directed electric currents on a dielectric-coated PEC circular cylinder as a function of α and for several distances s, with $\varepsilon_r = 2$, $\mu_r = 1$, $b = 5\lambda_0$, $d = 0.05\lambda_0$, $W = 0.1\lambda_0$ and $L = 0.1\lambda_0$.

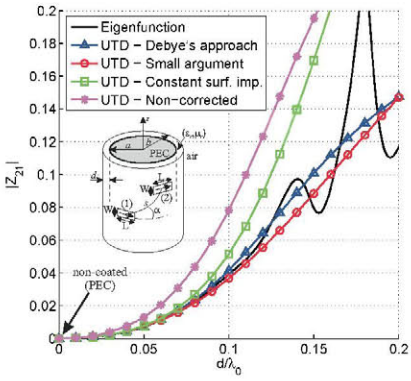

Fig. 6. Mutual impedance between two ϕ-directed electric currents on a dielectric-coated PEC circular cylinder as a function of d, with $\varepsilon_r = 2$, $\mu_r = 1$, $b = 5\lambda_0$, $W = 0.1\lambda_0$, $L = 0.1\lambda_0$, $s = 3\lambda_0$ and $\alpha = 40^{\circ}$.

surface ray angle is different from zero. If a dielectric layer is considered the TE surface impedance must be corrected for $z\phi'/\phi z'$ and $\phi\phi'$ source and field orientations, due to the torsion of surface rays around the cylinder. In the case of a uniform IBC cylinder the torsion effects are not present.

Three different surface impedance approaches are investigated, the so-called Debye's, small-argument and constant surface impedance approximation. First approach is the most accurate and is based on Debye's asymptotic approximation of Bessel functions, valid for thicknesses of substrate layer smaller than $0.15\lambda_0$. A planar approximation yields a small-argument expression valid for very large cylinders and coating thickness smaller than $0.1\lambda_0$, and its importance lies in the simplicity of the obtained surface impedance. These two surface impedance expressions depend on the spectral variables ν and k_z and are used inside Fock-type integrals in the UTD method. A constant surface impedance approach is obtained if ν is particularized with the first creeping wave pole on the complex ν-plane (an Elliot mode in some cases), since k_z depends only on the surface ray inclination. Even though the latter approach claims to be a surface impedance with a constant value (it only depends on the structure parameters), there is still the necessity for different TM and TE surface

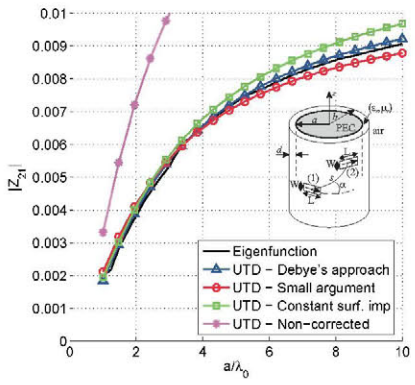

Fig. 7. Mutual impedance between two ϕ-directed electric currents on a dielectric-coated PEC circular cylinder as a function of a, with $\varepsilon_r = 2$, $\mu_r = 1$, $d = 0.05\lambda_0$, $W = 0.1\lambda_0$, $L = 0.1\lambda_0$, $s = 3\lambda_0$ and $\alpha = 40^o$.

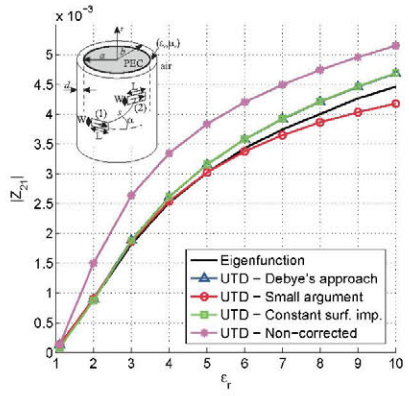

Fig. 8. Mutual impedance between two ϕ-directed electric currents on a dielectric-coated PEC circular cylinder as a function of ε_r, with $\mu_r = 1$, $b = 5\lambda_0$, $d = 0.02\lambda_0$, $W = 0.1\lambda_0$, $L = 0.1\lambda_0$, $s = 3\lambda_0$ and $\alpha = 40^o$.

impedances. This approach is valid for thin dielectric coatings (thinner than $0.07\lambda_0$), and its main drawback is the search of the root, which increases the computation time.

Unlike the formulations in [12], [13], which apply the asymptotic expansion to vector potentials and involve higher-order derivatives of Fock-type integrals to increase the precision, in the presented formulation there is not need to compute the latter functions which become complicated when a coating is present. Consequently, this approach is simpler and faster. The asymptotic Green's functions along with a MoM solver allow us to obtain mutual coupling of a circular cylindrical conformal array of patches or printed dipoles (the input impedance can be obtained through the eigenfunction solution). In order to extend this method for arbitrarily convex coated surfaces, it should be combined with the impedance sphere case, as shown in [7], but this issue needs to be investigated further.

ACKNOWLEDGMENT

The project has the support of the Spanish Ministry of Education, Culture and Sport under reference TEC2011-28789-C02-01, a Spanish Ministry of Economy and Competitiveness scholarship (FPI) under reference BES-2009-021462, and the E.T.S.I. Telecomunicacion.

REFERENCES

[1] L. Josefsson and P. Persson, *Conformal Array Antenna. Theory and Design*. Wiley Interscience, Hoboken, New Jersey, USA, 2006.

[2] Z. Sipus, M. Lanne, and L. Josefsson, "Moment method analysis of circular cylindrical array of waveguide elements covered with a multilayer radome," *IEE Proceedings on Microwaves, Antennas and Propagation*, vol. 153, no. 1, pp. 29 – 37, Feb. 2006.

[3] S. Raffaelli, Z. Sipus, and P.-S. Kildal, "Analysis and measurements of conformal patch array antennas on multilayer circular cylinder," *IEEE Transactions on Antennas and Propagation*, vol. 53, no. 3, pp. 1105–1113, Mar. 2005.

[4] Z. Sipus, N. Burum, S. Skokic, and P.-S. Kildal, "Analysis of spherical arrays of microstrip antennas using moment method in spectral domain," *IEE Proceedings on Microwaves, Antennas and Propagation*, vol. 153, no. 6, pp. 533 – 543, Dec. 2006.

[5] Q. Balzano and T. Dowling, "Mutual coupling analysis of arrays of apertures on cones," *IEEE Transactions on Antennas and Propagation*, vol. 22, no. 1, pp. 92 – 97, Jan. 1974.

[6] R. G. Kouyoumjian and P. H. Pathak, "A uniform geometrical theory of diffraction for an edge in a perfectly conducting surface," *Prococeedings of IEEE*, vol. 62, no. 11, pp. 1448–1461, Nov. 1974.

[7] P. H. Pathak and N. Wang, "Ray analysis of mutual coupling between antennas on a convex surface," *IEEE Transactions on Antennas and Propagation*, vol. 29, no. 6, pp. 911–922, Nov. 1981.

[8] P. Persson and R. G. Rojas, "High-frequency approximation for mutual coupling calculations between apertures on a perfect electric conductor circular cylinder covered with a dielectric layer: Nonparaxial region," *Radio Science*, vol. 38, no. 4, pp. 18.1 – 18.14, 2003.

[9] V. B. Ertürk and R. G. Rojas, "Efficient computation of surface fields excited on a dielectric-coated circular cylinder," *IEEE Transactions on Antennas and Propagation*, vol. 48, no. 10, pp. 1507–1516, Oct. 2000.

[10] G. N. Watson, "The diffraction of electric waves by the earth," *Proceedings of the Royal Society of London*, vol. 95, pp. 83–99, 1918.

[11] R. Paknys, "Evaluation of Hankel functions with complex argument and complex order," *IEEE Transactions on Antennas and Propagation*, vol. 40, no. 5, pp. 569 – 578, May 1992.

[12] Ç. Tokgöz and R. J. Marhefka, "A UTD based asymptotic solution for the surface magnetic field on a source excited circular cylinder with an Impedance Boundary Condition," *IEEE Transactions on Antennas and Propagation*, vol. 54, no. 6, pp. 1750–1757, Jun. 2006.

[13] B. Alisan, V. B. Ertürk, and A. Altintas, "Efficient computation of nonparaxial surface fields excited on a electrically large circular cylinder with an Impedance Boundary Condition," *IEEE Transactions on Antennas and Propagation*, vol. 54, no. 9, pp. 2559–2567, Sep. 2006.

[14] B. Alisan and V. B. Ertürk, "A high-frequency based asymptotic solution for surface fields on a source-excited sphere with an Impedance Boundary Condition," *Radio Science*, vol. 45, no. 5, Oct. 2010.

[15] Ç. Tokgoz, P. H. Pathak, and R. J. Marhefka, "An asymptotic solution for the surface magnetic field within the paraxial region of a circular cylinder with an Impedance Boundary Condition," *IEEE Transactions on Antennas and Propagation*, vol. 53, no. 4, pp. 1435 – 1443, Apr. 2005.

[16] V. B. Ertürk and R. G. Rojas, "Paraxial space-domain formulation for surface fields on a large dielectric coated circular cylinder," *IEEE Transactions on Antennas and Propagation*, vol. 50, no. 11, pp. 1577 – 1587, Nov. 2002.

[17] M. A. Leontovich, *Investigations on Radiowave Propagation, Part II*. Printing House of the Academy of Sciences, Moscow, Russia, 1948.

[18] T. B. A. Senior and J. L. Volakis, *Approximate boundary conditions in electromagnetics*. The Institution of Electrical Engineers, London, UK, 1995.

[19] P. H. Pathak, *Private communication*.

[20] M. Abramovitz and I. A. Stegun, *Handbook of Mathematical Functions*. Dover Publications, New York, USA, 1972.

[21] M. Marin and P. H. Pathak, "Calculation of the surface fields created by a current distribution on a coated circular cylinder," ElectroScience Laboratory, Dept. Electrical Engineering, Ohio State University, Tech. Rep. 721565-1, Apr. 1989.

[22] V. A. Fock, "Diffraction of radio waves around the Earth's surface," *Journal of Physics USSR*, vol. 9, pp. 256–266, 1945.

[23] R. Paknys and N. Wang, "Creeping wave propagation constants and modal impedance for a dielectric coated cylinder," *IEEE Transactions on Antennas and Propagation*, vol. 34, no. 5, pp. 674–680, May 1986.